Advanced corrosion protection for mild steel in acidic environments: The power of 3-imino-3*H*-benzo[*f*]chromene-2-carboxamide

H.H. Al-Doori,[1] M.A.I. Al-Hamid,[2] A.F. Mahmood,[3] A.A.H. Kadhum[4] and A.A. Alamiery[5]*

[1]*Al-Karkh University of Science, Baghdad P.O. Box: 10001, Baghdad, Iraq*
[2]*Energy and Renewable Energies Technology Center, University of Technology, Baghdad P.O. Box: 10001, Baghdad, Iraq*
[3]*Oil and Gas Engineering Department, University of Technology, Baghdad P.O. Box: 10001, Baghdad, Iraq*
[4]*Al-Ameed University College, P.O. Box: 56001, Karbala, Iraq*
[5]*Al-Ayen Scientific Research Center, Al-Ayen Iraqi University, AUIQ, An Nasiriyah, P.O. Box: 64004, Thi Qar, Iraq*
**E-mail: dr.ahmed1975@gmail.com*

Abstract

This research investigates the efficacy of 3-imino-3*H*-benzo[*f*]chromene-2-carboxamide (IB[*f*]CC) as a corrosion inhibitor for mild steel in hydrochloric acid. Through a combination of weight loss measurements and density functional theory (DFT) calculations, the results reveal an impressive inhibition efficiency of 91.6% at 303 K after five hours of immersion. Corrosion rates lower notably with growing immersion times (1, 5, 10, 24, and 48 hours), with inhibition efficiency stabilizing beyond 10 hours. Additionally, a moderate upward thrust in efficiency is found as the temperature increases from 303 to 333 K. Adsorption of the inhibitor on the steel surface follows the Langmuir isotherm, suggesting a blended mode of physical and chemical adsorption. DFT calculations suggest sturdy interactions between the inhibitor's useful functional groups lactone, benzene rings, amino, carbonyl, and imino – with iron atoms, resulting in a stable protecting layer. The findings highlight IB[*f*]CC as a promising candidate for reinforcing the corrosion resistance of mild steel in acid-resistant materials used in industrial applications.

Received: November 22, 2024. Published: March 29, 2025 doi: 10.17675/2305-6894-2025-14-1-24

Keywords: *corrosion, density functional theory, Langmuir, immersion time, mass loss.*

1. Introduction

Corrosion of metals, especially mild steel, is a substantial issue in diverse industries, in particular the ones exposed to acidic environments. Mild steel, extensively used for its mechanical properties and value-effectiveness, is at risk of degradation in acidic solutions, including HCl [1, 2]. This degradation ends in monetary losses, structural failures, and

expanded renovation fees. Acidic media are generally used in industrial processes like pickling, descaling, and acid cleaning, further heightening the need for effective corrosion protection techniques. Inhibitors that may mitigate or prevent the corrosive attack of acids on mild steel surfaces are hence of paramount significance [3, 4]. Organic corrosion inhibitors, especially those containing heteroatoms (*e.g.*, nitrogen, sulfur, and oxygen), are known to be effective in reducing metallic degradation in acidic media. Adsorption of these inhibitors with the metal surface effectively hinders the corrosive agents by forming a protective film [5]. Among the various organic compounds examined, benzo[*f*]chromene derivatives stand out in terms of structural versatility and functional-groups beneficial for adsorption. The IB[*f*]CC is clearly impressive as a very good corrosion-inhibition agent, thanks to its almost perfectly shaped configuration that presents sites from the active lactone and benzene rings, as well as from amino, carbonyl, and imino groups all together. To assess corrosion resistance, the efficiency of this inhibitor in an HCl medium must be evaluated to enhance mild steel protection.

Corrosion for mild steel occurs in acidic media where it remains a regular problem for the industrial applications [6, 7]. Traditional corrosion inhibitors may be inadequate in harsh conditions or might also include environmental and value-related drawbacks [8]. This study addresses the need for an effective, sustainable, and dependable inhibitor which could significantly reduce the corrosion rate of mild metallic in hydrochloric acid. Despite existing studies on organic inhibitors, there may be limited research on the particular effects and performance of IB[*f*]CC. The lack of know-how at the adsorption mechanisms, structural properties, and inhibition overall performance of this compound limits its business applicability.

Can IB[*f*]CC function an effective corrosion inhibitor for mild steel in hydrochloric acid, and what are the mechanisms contributing to its performance? Corrosion inhibition has been considerably studied, with organic inhibitors regularly referred to their performance in acidic environments [9]. Organic molecules containing nitrogen, oxygen, and sulfur atoms can donate electrons to vacant d-orbitals of iron, establishing a defensive adsorption layer on steel surfaces [10]. The adsorption of inhibitors usually follows isotherms, consisting of the Langmuir or Freundlich isotherm, which describe the connection between inhibitor awareness and surface coverage [11]. Studies have shown that chromene-based compounds exhibit exceptional corrosion inhibition efficiency due to their π-electron systems and functional groups [10, 12]. Research through Guo *et al.* (2023) established that benzo[*f*]chromene can achieve high inhibition performance because of robust adsorption onto metallic surfaces, mediated with the aid of useful functional groups that offer binding sites [13]. Density functional concept (DFT) calculations in corrosion research offer a theoretical framework for expertise the interactions between inhibitor molecules and metal atoms [14, 15]. This approach has been used to assess electron density, molecular orbital distribution, and different properties, which offer insights into the inhibitory mechanism. Experimental methods such as weight loss measurements, electrochemical impedance spectroscopy (EIS), and potentiodynamic polarization exams were broadly used to assess

inhibitor performance [16, 17]. Weight loss measurements are in particular applicable as they at once suggest modifications in metallic loss over time [18, 19], at the same time as EIS and polarization checks assist determine the inhibitor's effect on anodic and cathodic methods [20]. Despite those findings, limited studies have centered especially on the usage of IB[*f*]CC as a corrosion inhibitor. Existing literature does no longer sufficiently cover the adsorption characteristics, performance balance across varying temperatures, and combined physical-chemical adsorption mechanisms of this compound. Investigating its effectiveness in HCl and exploring adsorption conduct using DFT can bridge this understanding gap and offer a foundation for future industrial applications [21, 22].

The aim of the current investigation is to assist the corrosion inhibitive performance of IB[*f*]CC for mild steel in HCl solution and to understand the mechanisms underlying its adsorption and protective characteristics. Experimental and theoretical techniques seek to identify the IB[*f*]CC's effectiveness and the functional groups that contribute to its adsorption on steel substrate. The research objectives can be summarized as follows:

1. To determine the corrosion inhibition efficiency of IB[*f*]CC for mild steel in hydrochloric acid solutions across varied immersion times;
2. To analyze the impact of temperature on inhibition efficiency and to assess the stability of the compound's performance across a temperature range of 303–333 K;
3. To investigate the adsorption behavior of the inhibitor on mild steel surfaces and validate whether it follows the Langmuir adsorption isotherm;
4. To perform density functional theory (DFT) calculations for insights into the molecular interactions and electronic properties that contribute to inhibitor effectiveness;
5. To evaluate the contribution of specific functional groups (*e.g.*, lactone, benzene rings, amino, carbonyl, and imino groups) in enhancing the inhibitor's performance by forming a stable protective film on the steel surface;
6. To provide recommendations for industrial applications of this inhibitor in acidic environments, contributing to improved material longevity and reduced maintenance costs.

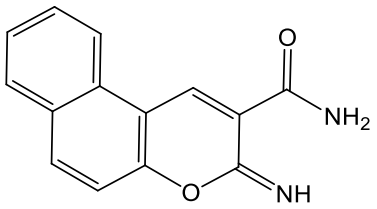

Figure 1. The chemical structure of IB[*f*]CC.

2. Experimental Details

2.1. Materials

The study utilized mild steel with a specific chemical composition: 0.21 wt.% carbon (C), 0.005 wt.% manganese (Mn), 0.38 wt.% silicon (Si), 0.05 wt.% sulfur (S), 0.01 wt.% aluminum (Al), and 0.09 wt.% phosphorus (P), with the remainder being iron (Fe). The

corrosion inhibition effectiveness of IB[*f*]CC was tested in a 1 M hydrochloric acid (HCl) environment. Steel samples, cut to dimensions of 4.0 cm×2.5 cm×0.1 cm, were used for the experiments. To prepare the surfaces, each sample was polished sequentially with abrasive papers of different grit sizes (400, 600, and 1200), achieving a smooth, uniform finish. The polished samples were then washed with double-distilled water, followed by an ethanol rinse to ensure all residues were removed. After drying at room temperature, the initial dry weight of each sample was recorded for later comparison [23, 24].

2.2. Preparation of hydrochloric acid solutions

To create a 1 M HCl solution, analytical-grade hydrochloric acid (37% purity) sourced from Merck, Malaysia, was diluted with double-distilled water. To assess the inhibitory effect of IB[*f*]CC, varying concentrations of the compound were dissolved in this HCl solution, ensuring thorough mixing for homogeneous distribution.

2.3. Weight loss measurements

The weight loss method was employed to quantify corrosion rates and evaluate the inhibition efficiency of IB[*f*]CC on mild steel in 1 M HCl. Polished samples, each with a 1 cm^2 exposed surface area, were immersed in 500 mL of the acid solution in glass beakers. The IB[*f*]CC inhibitor was tested at concentrations ranging from 0.1 mM to 1 mM, and experiments were conducted at temperatures between 303 K and 333 K, controlled with a thermostatic water bath [24, 25]. At immersion intervals of 5, 10, 24, and 48 hours, each sample was removed, rinsed with ultrapure water and ethanol using an ultrasonic cleaner, dried, and weighed to measure weight loss. The collected data allowed calculations of corrosion rate, inhibition efficiency, and surface coverage [26, 27]. Figure 2 illustrates the setup used to measure the corrosion of mild steel in 0.1 M HCl solution. The steel sample, with a polished surface, is suspended in the solution using a wire, and the entire setup is contained in a glass beaker.

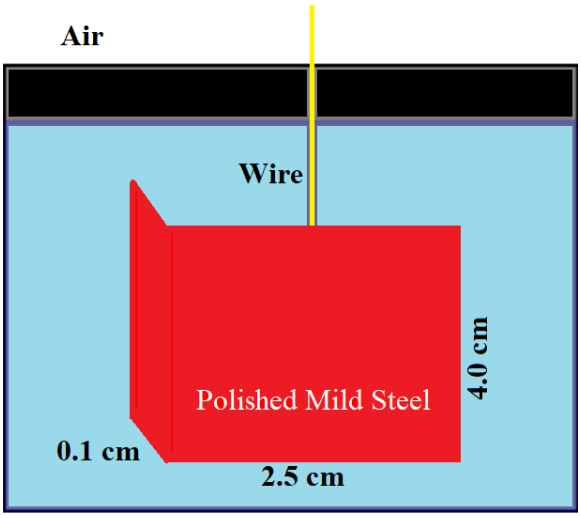

Figure 2. Experimental setup for weight loss corrosion test.

The corrosion rate (C_R) in milligrams per square centimeter per hour ($mg \cdot cm^{-2} \cdot h^{-1}$), inhibition efficiency (*IE*%), and surface coverage (θ) were determined using these equations (1–3):

$$C_R = \frac{W}{at} \tag{1}$$

W is the weight loss in grams, *a* is the exposed surface area of the steel sample (cm^2), and *t* is the immersion time (hours).

$$IE\% = \left[1 - \frac{C_{R(i)}}{C_{R(0)}}\right] \cdot 100 \tag{2}$$

where: $C_{R(0)}$ is the corrosion rate without the inhibitor (control), $C_{R(i)}$ is the corrosion rate with the inhibitor.

$$\theta = 1 - \frac{C_{R(i)}}{C_{R(0)}} \tag{3}$$

These formulas provided a detailed assessment of IB[*f*]CC's performance in reducing corrosion, calculated from the weight loss measurements. The study adhered to NACE standards for corrosion research, validating the reliability of the gravimetric approach in measuring inhibitor efficiency [24].

2.4. Theoretical study

Quantum chemical calculations were carried out using GAMESS software to analyze the inhibitor's electronic properties. The molecular structure of IB[*f*]CC was optimized at the DFT-B3LYP/6–31G(d) level [28]. Key quantum parameters were calculated, including the highest occupied molecular orbital (HOMO) energy, the lowest unoccupied molecular orbital (LUMO) energy, and other indices related to reactivity (4–8):

Ionization potential (*I*): $$I = -E_{HOMO} \tag{4}$$

Electron affinity (*A*): $$A = -E_{LUMO} \tag{5}$$

Electronegativity (χ): $$\chi = \frac{I + A}{2} \tag{6}$$

Chemical hardness (η): $$\eta = \frac{I - A}{2} \tag{7}$$

Chemical softness (σ): $$\sigma = \eta^{-1} \tag{8}$$

The electron transfer fraction (Δ*N*) between the inhibitor and the mild steel surface was also computed based on equation (9):

$$\Delta N = \frac{7 - \chi_{inh}}{2\eta_{inh}} \quad (9)$$

where χ_{inh} and η_{inh} refer to the electronegativity and hardness of the inhibitor, respectively. For these calculations, the reference values for iron (Fe) were taken as χ_{Fe}=7 eV and η_{Fe}=0 eV.

These theoretical characteristics provided insights into the electronic interactions between the tested inhibitor molecules and the iron atoms located on the steel surface, elucidating the mechanisms that improves corrosion impedance.

3. Results and Discussion

3.1. Weight loss measurements

3.1.1. Effect of inhibitor concentration

The impact of IB[*f*]CC concentration at the corrosion rate and inhibition efficiency (*IE*%) for steel in a 1 M HCl solution at 303 K is proven in Figure 3. As the inhibitor concentration multiplied from 0.1 mM to 0.5 mM, there has been a considerable decrease within the corrosion rate, followed through a corresponding enhancement in inhibition performance. The highest *IE*% of 91.6% become determined at an IB[*f*]CC concentration of 0.5 mM, indicating a strong inhibitory effect. The facts advocate that IB[*f*]CC acts as a powerful corrosion inhibitor, and its performance improves with growing concentration. This conduct is attributed to the better coverage of the inhibitor molecules on the metallic surface at better concentrations, which creates a defensive barrier that hinders the penetration of corrosive species to the steel surface. The discovered fashion aligns with the concepts of adsorption, where an increase in inhibitor concentration results in an extra wide variety of adsorbed molecules, thereby improving surface coverage and corrosion protection [27, 28].

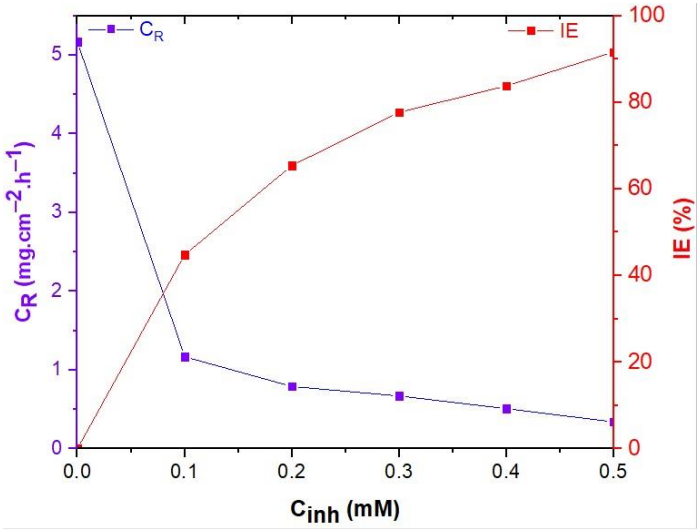

Figure 3. Effect of IB[*f*]CC concentration on corrosion rate (C_R) and inhibition efficiency (*IE*%) for mild steel in 1 M HCl solution at 303 K.

3.1.2. Effect of immersion time

Figure 4 suggests the effect of immersion time on the corrosion rate and inhibition performance at numerous concentrations of IB[*f*]CC. It is obvious that corrosion rate decreases with prolonged immersion time, at the same time as inhibition performance indicates a progressively increases reaching a stabilized state after approximately 5 hours. The results indicate that IB[*f*]CC adsorbs onto the mild steel surface over time, with more and more inhibitor molecules forming a dense shielding film. As immersion time progresses, the inhibitor achieves greater surface coverage, enhancing its effectiveness. This time-dependent behavior demonstrates that IB[*f*]CC can provide extended corrosion protection in acidic environments [29].

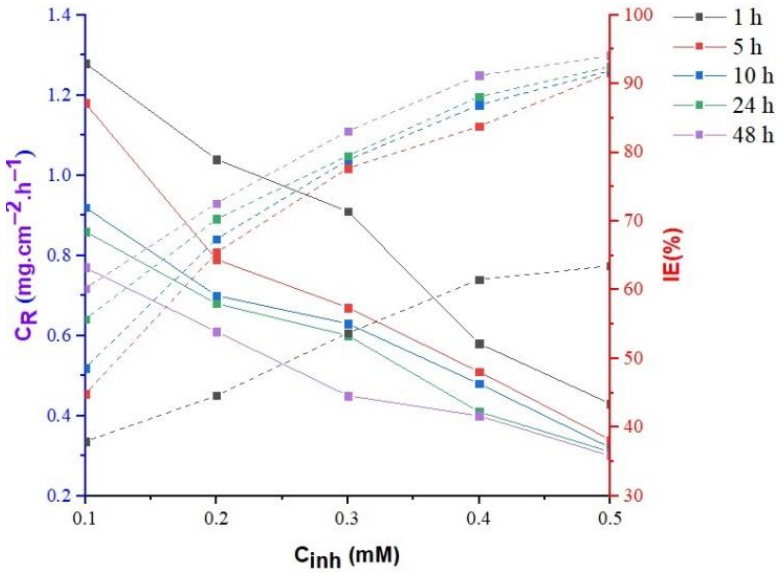

Figure 4. Effect of IB[*f*]CC concentration and immersion time on corrosion rate and inhibition efficiency.

3.1.3. Effect of temperature

The effect of temperature on the inhibition efficiency of IB[*f*]CC was studied across the temperature range of 303–333 K, as shown in Figure 5. The results show a steady rise in inhibition efficiency with increasing temperature, indicating that IB[*f*]CC remains effective at higher temperatures. The increase in *IE*% with temperature could be due to enhanced adsorption of the inhibitor at higher temperatures, leading to stronger interactions between the inhibitor molecules and the metal surface. This behavior supports the concept of chemisorption, where chemical bonding between the inhibitor and the metal surface intensifies with increasing temperature. However, the stability of the corrosion rate at higher temperatures suggests that IB[*f*]CC provides consistent protection, making it suitable for high-temperature applications [30].

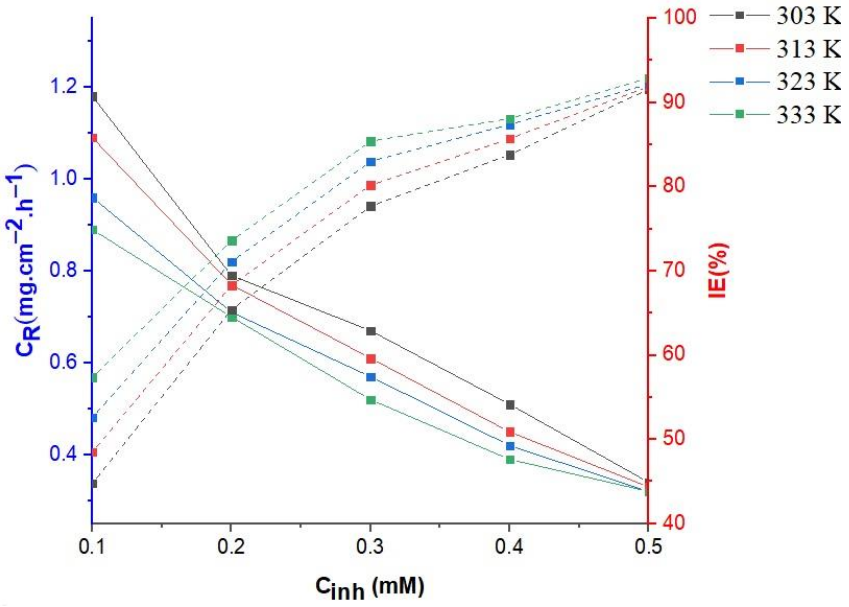

Figure 5. Effect of temperature on IB[*f*]CC inhibition efficiency and corrosion rate.

3.2. Adsorption isotherm

The adsorption of IB[*f*]CC on the metallic surface was analyzed using various adsorption isotherms. The Langmuir adsorption isotherm provided an excellent fit for the experimental data, as indicated by the high correlation coefficient (R^2=0.9985), as shown in Figure 6. It is suggested that IB[*f*]CC forms a stable, homogeneous, and protective layer on the metallic surface of the metal. The key parameters from the Langmuir equation, namely, *m* and *b*, *i.e.*, the slope and intercept, are 0.816 and 0.1427 respectively, which confirm that IB[*f*]CC forms a protective layer. This agent was weakly adsorbed on the surface of mild steel at room temperature. Its interaction with the surface could be attributed to electronic charges. In order to provide more specific details of IB[*f*]CC's interaction with mild steel, this work was conducted by fitting data of initial concentration of the adsorbate taken as [IB[*f*]CC] (range 0.8055 to 1.4077 mM) into various adsorption models such as the Langmuir, the Freundlich, and the Temkin isotherms. The correlation coefficients obtained were then compared to determine the suitability of the adsorption model. The data suggest that the adsorption of IB[*f*]CC is best described by the Langmuir isotherm with a high correlation coefficient of 0.9985 according to the R^2 values, related to the monolayer adsorption mechanism with a uniform value of energy. On the other hand, Freundlich and Temkin models, according to their correlation coefficients, were less favorable to be used in analyzing and understanding the adsorption behavior in this system. Table 1 provides the data, which provided quantifiable justification for the choice of the Langmuir model as the most appropriate for the phenomenon under scrutiny.

Table 1. Adsorption isotherm models and their correlation coefficients for IB[*f*]CC adsorption on mild steel.

Adsorption isotherm model	Equation	R^2	Adsorption characteristics
Langmuir isotherm	$\frac{C_{inh}}{\theta} = \frac{1}{K_L} + C_{inh}$	0.9985	Best fit; suggests monolayer adsorption on uniform active sites.
Freundlich isotherm	$\log\theta = \log K_F + \left(\frac{1}{n}\right)\log C_{inh}$	0.8723	Poor fit; suggests heterogeneous surface adsorption but not dominant in this system.
Temkin isotherm	$\theta = B\ln K_T C_{inh}$	0.8431	Poor fit; suggests weak inhibitor-metal interactions.

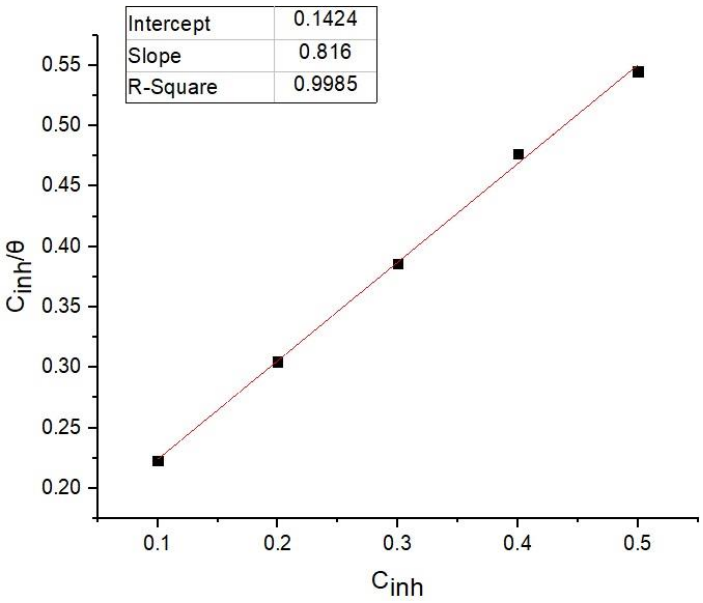

Figure 6. Langmuir adsorption isotherm for IB[*f*]CC on mild steel.

3.3. Quantum chemical calculations

Quantum chemical calculations offer crucial insights on the electronic structure and reactivity of the IB[*f*]CC molecule, which are essential for understanding its performance as a corrosion inhibitor. By considering the parameters together with the highest-occupied molecular orbital (HOMO) and the lowest unoccupied molecular orbital (LUMO) energies, *i.e*., energy gap (ΔE_{gap}), electronegativity (χ), hardness (η), softness (σ), and nucleophilicity (ΔN), the electron-donation capability or effective adsorption of the molecule on a mild steel surface, *etc*., can be explained (32). As shown in Figure 7, the HOMO-LUMO energies of IB[*f*]CC fluctuates to indicate the capability of the molecule to donate and accept electrons,

respectively. The HOMO energy (E_{HOMO}=−11.65 eV) reveals the ability of the molecule to donate electrons and adsorb onto the mild steel surface *via* interaction with the empty d-orbitals of iron atoms. In contrast, The LUMO energy of −5.148 eV suggests its electron-accepting ability that allows electrons to be drawn by the molecule from the metal. This characteristic is noted to be beneficial for molecular stabilization on the metal and for ensuring protection.

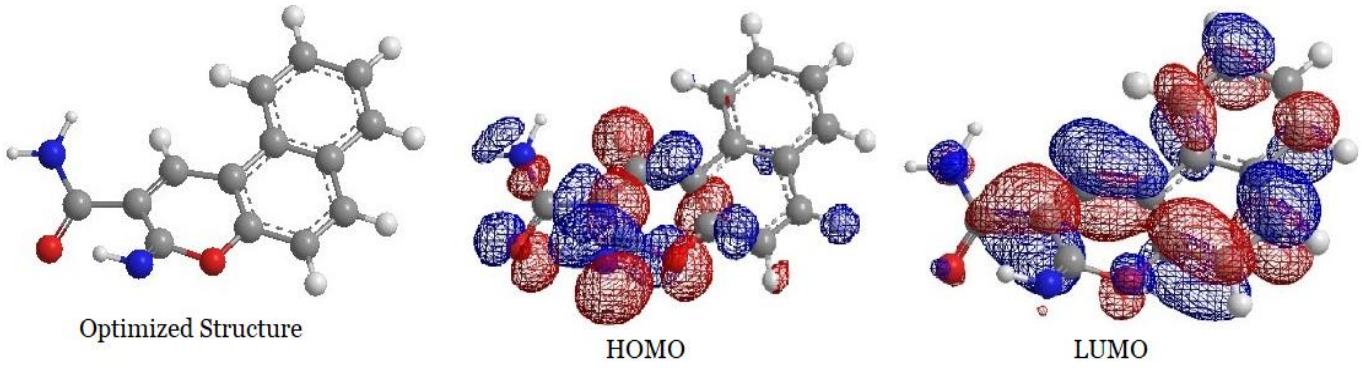

Figure 7. Optimized structure, HOMO, and LUMO of IB[*f*]CC.

Gap energy has critical importance in determining the reactivity of the inhibitor. The smaller ΔE_{gap} means higher chemical reactivity, making it easier for the molecule to interact with the metal surface. For IB[*f*]CC the calculated quantum chemistry gap is moderate, indicating a balance between stability and reactivity, a favorable condition for adsorbing and gaining a thin protective layer on the metallic surface [33]. Table 2 provides a compilation of critical parameters for the molecule observed through quantum chemistry calculations. Observations obtained for the ionization potential (I), electron affinity (A), electronegativity (χ), chemical hardness (η), chemical softness (σ), and electron transfer fraction (ΔN) allow one to analyze the molecule's reactivity and tendency to interact with the metal surface. I and A were obtained from the E_{HOMO} and E_{LUMO}, which refer to the molecule's acceptance of electrons and donation of electrons, respectively. Elucidated above, while the electronegativity (χ) portrays the attracting ability of the molecule for electrons, higher electronegativity enhances an extra attraction towards the steel-surface electrons and further enhances adsorption. Chemical hardness (η) and Chemical softness (σ) determine the stability or reactivity levels of the molecule, while greater softness further enhances reactivity for efficient adsorption onto the metal. Electron transfer fraction (ΔN) represents the charge transfer between the inhibitor and the metallic surface. An advantageous ΔN shows electron donation from the inhibitor to the metallic, which contributes to the adsorption procedure.

Table 2. Quantum chemical parameters of IB[*f*]CC.

Parameter	Value
Ionization potential (*I*), (eV)	11.65
Electron affinity (*A*), (eV)	5.148
HOMO energy (eV)	–11.65
LUMO energy (eV)	–5.148
Energy gap (eV)	6.502
Electronegativity (χ), (eV)	8.399
Chemical hardness (η), (eV)	3.251
Chemical softness (σ), (eV^{-1})	0.3075
Electron transfer fraction (Δ*N*)	1.177

Mulliken charge analysis offers data about the distribution of electron density in the IB[*f*]CC molecule, which affects its interplay with the metallic surface. Atoms with excessive negative charges, consisting of nitrogen and oxygen (Table 3), are likely energetic sites for adsorption because of their electron-rich nature, promoting strong interactions with the positively charged regions on the steel surface.

Table 3. Mulliken charge analysis of IB[*f*]CC.

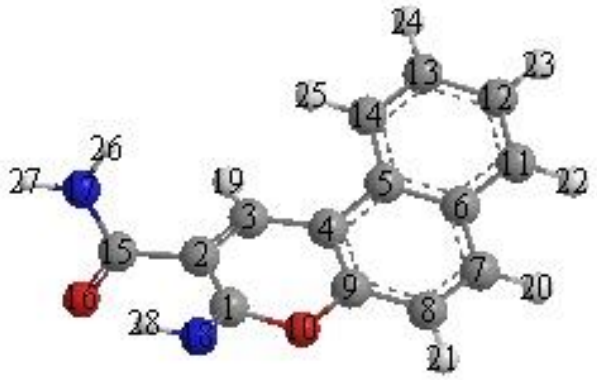

Atom	Mulliken charge
C (1)	0.2179
C (2)	–0.2139
C (3)	0.0998
C (4)	–0.1711
C (5)	0.0342
C (6)	–0.0775

Atom	Mulliken charge
C (7)	0.0158
C (8)	–0.0824
C (9)	0.1846
O (10)	–0.1805
C (11)	–0.0222
C (12)	–0.0678
C (13)	–0.0327
C (14)	–0.0653
C (15)	0.4036
O (16)	–0.3504
N (17)	–0.4165
N (18)	–0.2448

The quantum chemical calculations support the experimental findings that IB[*f*]CC acts as an effective corrosion inhibitor. The negative HOMO energy indicates a high electron-donating capacity, which facilitates the formation of a protective adsorption layer on the steel surface. Additionally, the moderate energy gap suggests that IB[*f*]CC possesses optimal reactivity to interact with the metal, while still maintaining structural stability. The presence of electronegative atoms, particularly nitrogen and oxygen, provides sites for chemical interaction with the steel surface, as indicated by the Mulliken charge analysis.

3.4. Suggested inhibition mechanism

The inhibition mechanism of IB[*f*]CC as a corrosion inhibitor for mild steel in hydrochloric acid (HCl) solutions can be understood through multiple interdependent processes. These include adsorption on the metal surface, formation of a protective layer, inhibition of both anodic and cathodic reactions, influence of the electronic properties of the inhibitor, and possible synergistic effects.

1. Adsorption on the metal surface

The adsorption of IB[*f*]CC is hypothesized to involve both chemisorption and physisorption, primarily based on the molecule's electronic structure and functional groups [32]. Chemisorption occurs when a strong chemical bond forms between the inhibitor molecules and the metal surface. For IB[*f*]CC, chemisorption is facilitated by the presence of electronegative atoms including nitrogen and oxygen, which could donate electrons to the iron atoms on the metallic surface. This electron-sharing interaction results in the formation of a covalent bond, strengthening the adsorption and enhancing the steadiness of the protecting layer. Density functional theory (DFT) analysis reveals high electron density on

nitrogen and oxygen atoms, facilitating this adsorption process. The π-electrons can interact with the iron d-orbitals, creating a physical attraction that enhances surface coverage. Although weaker than chemisorption, physisorption enables rapid initial adsorption, which then transitions into stronger chemisorptive bonds, providing a comprehensive protective effect.

2. Formation of a protective layer

After adsorption, IB[*f*]CC develops a protective layer on the mild steel surface, serving as a physical barrier against the corrosive HCl solution. This layer acts as a physical barrier, keeping apart the metallic surface from the corrosive HCl solution. The planar shape and the presence of functional groups (like lactone, imino, and carbonyl groups) in IB[*f*]CC enhance the molecule's ability to spread across and cling to the metal surface, resulting in a dense, cohesive layer [33]. This layer effectively blocks hydrogen and chloride ions, which are responsible for initiating and accelerating corrosion. By preventing their interaction with the metal, the inhibitor effectively reduces the corrosion rate. The combination of physisorption and chemisorption allows IB[*f*]CC to form a layer that is both stable and adherent, providing long-term corrosion protection [34].

3. Inhibition of anodic and cathodic reactions

Anodic reactions in acidic environments involve the dissolution of iron ($Fe \rightarrow Fe^{2+} + 2e^-$). IB[*f*]CC inhibits this mechanism by using adsorbing onto anodic sites at the metal surface, thereby reducing the rate at which iron ions are released into solution. This effect is largely due to the strong chemisorption interplay among the inhibitor molecules and the anodic sites, which blocks these energetic regions and suppresses the dissolution of iron. The formation of a solid layer through chemisorption, as discussed earlier, guarantees that the inhibitor stays powerful in preventing iron dissolution, even when exposed to higher temperatures or extended immersion times. Cathodic reactions in acidic media often involve the discount of hydrogen ions ($2H^+ + 2e^- \rightarrow H_2$). IB[*f*]CC inhibits this response with the aid of blocking the sites in which hydrogen ions are reduced, thereby lowering the supply of electrons for hydrogen evolution. The functional groups in IB[*f*]CC, particularly nitrogen-containing ones, can accept protons, reducing the likelihood of hydrogen evolution on the metal surface [35]. Additionally, physisorption contributes to blocking off cathodic sites, which facilitates to decrease rate of the cathodic reaction, lowering the manufacturing of hydrogen evolution and mitigating corrosion [36].

4. Role of electronic properties

Electronic properties of IB[*f*]CC play a vital role in its inhibition efficiency. As proven *via* quantum chemical calculations, IB[*f*]CC has optimal HOMO-LUMO energy gap, which indicates a balance between stability and reactivity. The excessive HOMO strength suggests that IB[*f*]CC can effectively donate electrons to the metal surface, that is critical for forming

a strong chemisorption bond [37]. The Mulliken charge analysis discovered that oxygen and nitrogen atoms in the IB[*f*]CC molecule exhibits high reactivity, making these atoms energetic sites for adsorption at the undoubtedly charged metallic surface. These electronic interactions enhance the molecule's adsorption ability, contributing to the formation of a dense, solid layer that impedes both anodic and cathodic reactions. Additionally, ΔN calculation shows that IB[*f*]CC donates electrons to the metal surface, reinforcing its interplay with the metal, which supports the adsorption technique, mainly chemisorption.

5. Synergistic effects

The inhibition efficiency of IB[*f*]CC is further enhanced by the combined effect of its functional groups, which collectively contribute to its protective performance. The functional groups, in particular lactone, benzene rings, imino, amino, and carbonyl, allow the molecule to interact with the metal surface at multiple adsorption sites. This multi-factor attachment strengthens the adsorption and complements the uniformity of the protecting layer [31, 33]. Furthermore, the conjugated structure of IB[*f*]CC, with π-electron structures in the benzene rings, allows for π-d interactions with iron atoms, adding an extra layer of adsorption strength. This synergistic impact between unique functional groups and structural elements in IB[*f*]CC maximizes surface coverage, improves layer stability, and ensures a consistent inhibition impact throughout varying temperatures and immersion times. The inhibition mechanism of IB[*f*]CC on metal in HCl involves multiple synergistic mechanisms to reduce corrosion. Adsorption, each through chemisorption and physisorption, bureaucracy the idea of safety, main to the formation of a dense, protective layer. This layer prevents penetration of corrosive ions to the steel surface and disrupts anodic and cathodic reactions, appreciably reducing the corrosion rate. The electronic properties of IB[*f*]CC, blended with synergistic effects from its functional groups, beautify adsorption strength and coverage, making IB[*f*]CC an effective and durable inhibitor for metal in acidic environments. Based on Figure 9, IB[*f*]CC molecules are adsorbed onto the metal surface *via* both chemisorption (strong bonding through nitrogen and oxygen atoms) and physisorption (weaker interactions, probably *via* π-electrons in benzene rings).

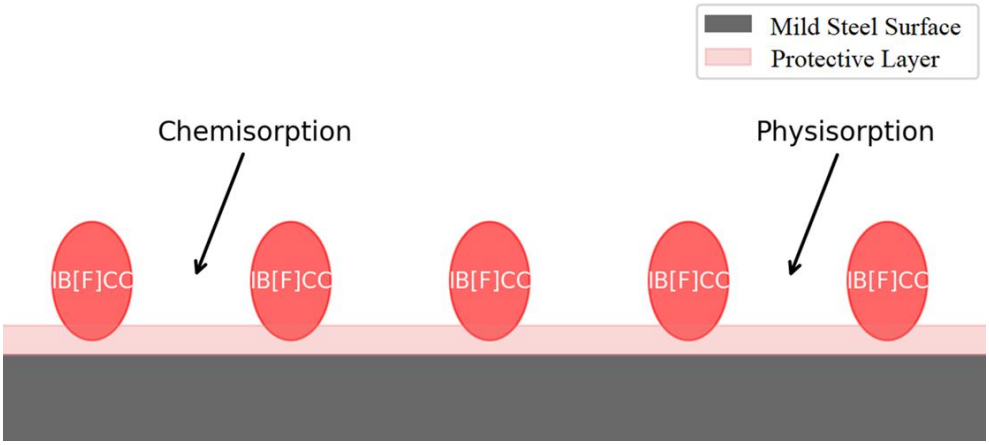

Figure 9. Mechanism of IB[*f*]CC corrosion inhibition on mild steel surface.

The inhibition efficiency of a corrosion inhibitor is closely tied to its adsorption behavior on the metal surface, which can occur through either physisorption or chemisorption. These two distinct adsorption mechanisms influence different electrochemical processes, namely the hydrogen evolution reaction (HER) and anodic dissolution, in unique ways. Physisorption involves weak interactions, such as Van der Waals forces or electrostatic attraction, between the inhibitor molecules and the metal surface. This type of adsorption is typically reversible and does not involve significant electron transfer. When an inhibitor undergoes physisorption, it physically blocks the active sites on the metal surface, thereby reducing the availability of sites for proton reduction during HER. In contrast, chemisorption involves the formation of strong chemical bonds (covalent or ionic) between the inhibitor molecules and the metal surface, accompanied by significant electron transfer. This process is often irreversible and leads to the formation of a stable protective layer on the surface. Chemisorption effectively alters the electronic properties of the metal surface, thereby inhibiting the anodic dissolution process.

DFT can provide additional insights into adsorption mechanisms by modeling the electronic interactions between the inhibitor and the metal surface. Physisorption is characterized by low adsorption energy and minimal charge transfer, whereas chemisorption exhibits high adsorption energy and significant electron exchange. Analysis of the HOMO-LUMO gap and charge distribution further supports the distinction between these two adsorption processes.

3.5. Comparison of IB[f]CC with other published corrosion inhibitors

To comprehensively evaluate the overall performance of IB[*f*]CC as a corrosion inhibitor, it's miles important to evaluate its inhibition performance, effectiveness throughout one of a kind corrosive media, compatibility with diverse metals, and adsorption mechanisms with different broadly studied inhibitors. This evaluation facilitates function IB[*f*]CC inside the broader context of corrosion inhibition studies and assesses its ability advantages and barriers relative to other inhibitors. Table 4 presents a comparative analysis of IB[*f*]CC's performance relative to other well-studied corrosion inhibitors, focusing on key factors such as the corrosive medium, optimum temperature, immersion time, inhibition efficiency, and adsorption mechanism.

Table 4. Comparative analysis of IB[*f*]CC with other published corrosion inhibitors.

Inhibitor type	Corrosive solution	Optimum temperature, (K)	Immersion time, (h)	Inhibition efficiency, (%)	Adsorption mechanism	Ref.
IB[*f*]CC	1 M HCl	303–333	5	91.6	Mixed (Physisorption & Chemisorption)	This Study
1-Phenylimidazole	1 M HCl	298–323	6	80–90	Chemisorption	[37]
Schiff base derivatives	0.5 M H_2SO_4	298–313	4	85–90	Chemisorption	[38]
Salicylic acid	1 M HCl	303–323	3	50–80	Physisorption	[39]
Benzotriazole	3.5% NaCl	298–323	12	75–85	Mixed	[40]

1. Inhibition efficiency

The inhibition efficiency of IB[*f*]CC, which reaches up to 91.6% at most suitable concentrations, is corresponding to or exceeds that of several properly-studied corrosion inhibitors, consisting of imidazole derivatives, Schiff bases, and organic acids. Each of these classes possesses specific functional groups and mechanisms that contribute to their effectiveness in reducing corrosion [37–39].

- **Imidazole derivatives**: Imidazole-primarily based compounds are widely recognized for their corrosion inhibition properties, specifically in acidic environments. Derivatives like 1-phenylimidazole typically achieve inhibition efficiencies of 80–90% in HCl. The nitrogen atoms inside the imidazole ring have interaction with the metallic surface, forming a stable adsorption layer. IB[*f*]CC matches or slightly exceeds the performance of many imidazole-based inhibitors owing to its superior electron-donating ability from multiple functional groups, which include nitrogen, oxygen, and π-electrons from benzene rings;
- **Schiff bases**: Schiff bases represent another class of effective corrosion inhibitors, especially those with heteroatoms like nitrogen and oxygen. These compounds generally attain inhibition efficiencies round 85–90% in acidic media. Schiff bases adsorb on steel surfaces *via* their azomethine (−C=N−) group, providing sturdy binding to the steel;
- While similar in efficiency, IB[*f*]CC offers additional functional groups, inclusive of lactone and carbonyl, which enhance its interaction with the metallic surface and offer slightly better inhibition efficiencies in a some cases;
- **Organic acids**: Organic acids, including benzoic acid and salicylic acid, are broadly used as corrosion inhibitors in each acidic and neutral environments. However, their inhibition efficiencies are usually ranges between 50–80% due to their particularly

simple molecular structures and weaker adsorption at the steel surface. Compared to those acids, IB[*f*]CC demonstrates advanced inhibition performance, as it has a greater complicated shape with a couple of adsorption sites, enhancing its ability to shape a sturdy shielding layer.

The high inhibition efficiency of IB[*f*]CC, driven by its unique structure with multiple electron-rich functional groups, makes it highly competitive with other corrosion inhibitors, particularly in acidic environments.

2. Corrosive solution type (acid vs. base)

The performance of corrosion inhibitors varies significantly between acidic and basic media, as the inhibitor's solubility, ionization, and adsorption behavior change with pH. Most organic inhibitors, including IB[*f*]CC, are optimized for acidic environments, where they demonstrate higher inhibition efficiencies [40, 41].

- **Acidic media**: IB[*f*]CC has been specifically studied in 1 M hydrochloric acid, an acidic medium where it shows strong inhibition efficiency. The acidic environment promotes protonation of the nitrogen atoms in the IB[*f*]CC molecule, which enhances its adsorption onto the steel surface through electrostatic interactions. This behavior aligns well with other inhibitors like imidazole derivatives and Schiff bases, which also perform optimally in acidic media. The similarity in performance in acidic solutions suggests that IB[*f*]CC could be used interchangeably with these other inhibitors for acid-based applications;
- **Basic media**: The performance of IB[*f*]CC in basic media has not been extensively studied. Generally, organic inhibitors like imidazole derivatives and Schiff bases are less effective in basic environments due to decreased adsorption strength. In basic media, metal surfaces are often passivated, reducing the effectiveness of organic inhibitors. Certain organic acids exhibit higher effectiveness in basic media due to their interaction with metal hydroxide layers. IB[*f*]CC may require modification or combination with other compounds to achieve similar efficiencies in basic solutions.

3. Metal type (steel vs. other alloys)

Corrosion inhibitors often show various effectiveness depending on the metal kind. While IB[*f*]CC is particularly studied for mild steel, understanding its potential performance on different metals and alloys affords insight into its broader applicability [42–44].

- **Mild steel**: IB[*f*]CC has been proven to offer high inhibition performance for mild steel in acidic environments. Its adsorption on steel surface is strong because of the interplay of nitrogen, oxygen, and π-electrons with iron atoms. This is similar to imidazole derivatives and Schiff bases, which additionally perform well on steel surfaces. The more than one adsorption sites in IB[*f*]CC permit it to efficiently cover the metal surface, thereby decreasing corrosion;

- **Stainless steel**: Stainless steel, alloyed with chromium and nickel, naturally forms a passive oxide layer that protects against corrosion in various environments. In acidic environments where the oxide layer is compromised, inhibitors like Schiff bases and imidazoles enhance corrosion resistance *via* adsorbing onto uncovered metallic sites. While IB[*f*]CC ought to probably be effective for stainless steel in acidic situations, its performance may differ from that on mild steel due to the preexisting passive layer;
- **Copper and aluminum alloys**: Copper and aluminum alloys exhibit different behavior from steel due to their unique electrochemical properties. Copper, for instance, naturally forms a stable oxide layer in environments, and natural inhibitors like benzotriazole generally more effective than imidazoles or Schiff bases. Aluminum alloys, on the other hand, are highly reactive in both acidic and basic solutions, and inhibitors that can form a stable complex with aluminum, such as organic phosphates, are often preferred. The benzene rings and nitrogen/oxygen functional groups in IB[*f*]CC may allow some level of adsorption on copper, but it is unlikely to match the efficiency observed on steel.

In summary, IB[*f*]CC shows great potential as a corrosion inhibitor for mild steel, particularly in acidic environments, but may not be as effective for other metals like copper and aluminum alloys, where alternative inhibitors may be preferred.

4. Adsorption mechanism

The adsorption mechanism of IB[*f*]CC, as discussed previously, involves both physisorption and chemisorption. Comparatively, other corrosion inhibitors also display characteristic adsorption behaviors influenced by their molecular structures [45, 46].

- **Imidazole and benzimidazole derivatives**: Imidazole and benzimidazole derivatives typically adsorb onto metal surfaces *via* the nitrogen atoms within their rings, forming a chemisorptive bond with the metal. This process is often characterized by strong covalent interactions that create a stable protective layer. Like IB[*f*]CC, these inhibitors rely on electron donation from nitrogen atoms for adsorption; however, IB[*f*]CC has additional functional groups that enhance adsorption through multiple interactions;
- **Schiff bases**: Schiff bases adsorb on metal surfaces through the azomethine (C=N) group, which provides a site for strong chemical bonding with metal atoms. This adsorption mechanism is highly effective in acidic media, similar to IB[*f*]CC, but may not involve the same level of multi-point adsorption due to fewer functional groups [47].

4. Conclusion

This study demonstrates that IB[*f*]CC is a highly effective corrosion inhibitor for mild steel in HCl environments. Through gravimetric analysis, quantum chemical calculations, and adsorption research, IB[*f*]CC has shown excellent inhibition performance, reaching 91.6%

at the highest studied concentration. The inhibitor's effectiveness is attributed to its precise molecular shape, which combines multiple functional groups including nitrogen, oxygen, and π-electron structures that facilitate strong adsorption onto the steel surface. IB[*f*]CC adsorption mechanism involves both chemisorption and physisorption, resulting in a strong and cohesive defensive layer that significantly reduces corrosion rates and inhibits both anodic and cathodic reactions. Compared to other organic inhibitors, including imidazoles, Schiff bases, and organic acid derivatives, IB[*f*]CC exhibits high inhibition efficiency in acidic solution, specifically for mild steel. Its electronic properties, confirmed through DFT calculations, highlight its robust electron-donating potential and balance, which enhance its adsorption strength and effectiveness. The inhibitor's overall performance is further enhanced by interactions among its functional groups, ensuring stability across various temperatures and immersion durations.

Funding Statement

This research was funded by Al-Ayen Iraqi University (AUIQ) under the program "Innovative Corrosion Inhibitors: A New Frontier in Materials Protection" (AUIQ-RFP2024-CI). The authors express their sincere gratitude for the financial support that made this study possible.

Acknowledgment

The authors would like to express their heartfelt gratitude to Al-Ayen Iraqi University (AUIQ) for providing the financial support under the research project titled "Innovative Corrosion Inhibitors: A New Frontier in Materials Protection" (Project Code: AUIQ-RFP2024-CI). Their assistance and resources were invaluable in the successful completion of this study.

References

1. F. Zhang, Y. Tang, Z. Cao, W. Jing, Z. Wu and Y. Chen, Performance and theoretical study on corrosion inhibition of 2-(4-pyridyl)-benzimidazole for mild steel in hydrochloric acid, *Corros. Sci*., 2012, **61**, 1–9. doi: 10.1016/j.corsci.2012.03.045
2. S.L.A. Kumar, M. Gopiraman, M.S. Kumar and A. Sreekanth, 2-Acetylpyridine-N(4)-Morpholine Thiosemicarbazone (HAcpMTSc) as a Corrosion Inhibitor on Mild Steel in HCl, *Ind. Eng. Chem. Res*., 2011, **50**, no. 13, 7824–7832. doi: 10.1021/ie200487g
3. H.M.A. El-Lateef, M.M. Khalaf, K. Shalabi and A.A. Abdelhamid, Efficient Synthesis of 6,7-Dihydro-5H-cyclopenta[b]pyridine-3-carbonitrile Compounds and Their Applicability As Inhibitor Films for Steel Alloy Corrosion: Collective Computational and Practical Approaches, *ACS Omega*, 2022, **7**, no. 28, 24727–24745. doi: 10.1021/acsomega.2c02639

4. C. Verma, M.A. Quraishi and K.Y. Rhee, Corrosion inhibition relevance of semicarbazides: electronic structure, reactivity and coordination chemistry, *Rev. Chem. Eng*., 2022, **39**, no. 6, 1005–1026. doi: 10.1515/revce-2022-0009
5. A.A. Altalhi, Anticorrosion Investigation of New Diazene-Based Schiff Base Derivatives as Safe Corrosion Inhibitors for API X65 Steel Pipelines in Acidic Oilfield Formation Water: Synthesis, Experimental, and Computational Studies, *ACS Omega*, 2023, **8**, no. 34, 31271–31280. doi: 10.1021/acsomega.3c03592
6. B.D.B. Tiu and R.C. Advincula, Polymeric Corrosion Inhibitors for the Oil and Gas Industry: Design Principles and Mechanism, *React. Funct. Polym*., 2015, **95**, 25–45. doi: 10.1016/j.reactfunctpolym.2015.08.006
7. M. Farsak, H. Keleş and M.A. Keleş, New Corrosion Inhibitor for Protection of Low Carbon Steel in HCl Solution, *Corros. Sci*., 2015, **98**, 223–232. doi: 10.1016/j.corsci.2015.05.036
8. S. Jagadeesan, F. Benhiba, A. Nagarajan, A. Zarrouk and S. Chitra, Thiazolo thiadiazole derivatives as anti-corrosion additives for acid corrosion, *Chem. Data Collect*., 2020, **26**, no. 4, 100358. doi: 10.1016/j.cdc.2020.100358
9. P. Muthukrishnan, B. Jeyaprabha and P. Prakash, Adsorption and corrosion inhibiting behavior of Lannea coromandelica leaf extract on mild steel corrosion, *Arabian J. Chem*., 2017, **10**, S2343–S2354. doi: 10.1016/j.arabjc.2013.08.011
10. Y.J. Qiang, H. Zhi, L. Guo, A. Fu, T. Xiang and Y. Jin, Experimental and molecular modeling studies of multi-active tetrazole derivative bearing sulfur linker for protecting steel from corrosion, *J. Mol. Liq*., 2022, **351**, 118638. doi: 10.1016/j.molliq.2022.118638
11. A. Al-Amiery, M.L. Shaker, A.A. Kadhum and M.S.Takriff, Synthesis, characterization and gravimetric studies of novel triazole-based compound, *Int. J. Low-Carbon Technol*., 2021, **15**, no. 2, 164–70. doi: 10.1093/ijlct/ctz067
12. H. Fakhry, M. El Faydy, M.E. Faydy, F. Benhiba, T. Laabaissi, M. Bouassiria, M. Allali, B. Lakhrissi, H. Oudda, A. Guenbour and I. Warad, A newly synthesized quinoline derivative as corrosion inhibitor for mild steel in molar acid medium: Characterization (SEM/EDS), experimental and theoretical approach, *Colloids Surf., A*, 2021, **610**, 125746. doi: 10.1016/j.colsurfa.2020.125746
13. B.A. Jahdaly and G.S. Masaret, Exploring the Potential of a Green Synthesized Chromene Derivative as an Inhibitor for Copper Corrosion in Acidic Environments: A Combined Experimental and Theoretical Investigation, *Arab. J. Sci. Eng*., 2024, Jul 19, 1–4. doi: 10.1007/s13369-024-09307-9
14. T. Guo, Y. Chen, W. Chen, S.J. Semple, G.X. Gu, S.W. Polyak, G. Sun, H. Venter and S. Ma, Design and synthesis of benzochromene derivatives as AcrB inhibitors for the reversal of bacterial multidrug resistance, *Eur. J. Med. Chem*., 2023, **249**, 115148. doi: 10.1016/j.ejmech.2023.115148
15. I.B. Obot, D.D. Macdonald and Z.M. Gasem, Density functional theory (DFT) as a powerful tool for designing new organic corrosion inhibitors. Part 1: an overview, *Corros. Sci*., 2015, **99**, 1–30.

16. D. Kumar, N. Jain, V. Jain and B. Rai, Amino acids as copper corrosion inhibitors: A density functional theory approach, *Appl. Surf. Sci*., 2020, **514**, 145905. doi: 10.1016/j.apsusc.2020.145905
17. A. Singh, K.R. Ansari, P. Banerjee, M. Murmu, M.A. Quraishi and Y. Lin, Corrosion inhibition behavior of piperidinium-based ionic liquids on Q235 steel in hydrochloric acid solution: experimental, density functional theory and molecular dynamics study, *Colloids Surf., A*, 2021, **623**, 126708. doi: 10.1016/j.colsurfa.2021.126708
18. A.F. Hamood, H.M. Habeeb, B.A. Abdulhussein, A.M. Mustafa, F.F. Sayyid, M.M. Hanoon, T.S. Gaaz, L.A. Hameed and A.A. Alamiery, Weight loss, electrochemical measurements, and DFT studies on corrosion inhibition by 7-mercapto-4-methylcoumarin, *Results Eng*., 2024, **23**, 102677. doi: 10.1016/j.rineng.2024.102677
19. K. Haruna and T.A. Saleh, Dopamine functionalized graphene oxide (DGO) as a corrosion inhibitor against X60 carbon steel corrosion in a simulated acidizing environment; An electrochemical, weight loss, SERS, and computational study, *Surf. Interfaces*, 2024, **44**, 103688. doi: 10.1016/j.surfin.2023.103688
20. L.C. Jing, W.H. Geng, Z.L. Bao, P.F. Qian, R.Y. Chang, T.Y. Li, Y.L. Guo, D. Zhang and H.Z. Geng, Synthesis of polyaniline tannate-modified carbon nanotubes by oxidative copolymerization as highly efficient corrosion inhibitors for mild steel in HCl solution, *J. Colloid Interface Sci*., 2025, **680**, Part A, 479–495. doi: 10.1016/j.jcis.2024.10.189
21. A. Mishra, J. Aslam, C. Verma, M.A. Quraishi and E.E. Ebenso, Imidazoles as Highly Effective Heterocyclic Corrosion Inhibitors for Metals and Alloys in Aqueous Electrolytes: A Review, *J. Taiwan Inst. Chem. Eng*., 2020, **114**, 341–358. doi: 10.1016/j.jtice.2020.08.034
22. S.K. Saha, M. Murmu, N.C. Murmu and P. Banerjee, Evaluating electronic structure of quinazolinone and pyrimidinone molecules for its corrosion inhibition effectiveness on target specific mild steel in the acidic medium: a combined DFT and MD simulation study, *J. Mol. Liq*., 2016, **224**, 629–638. doi: 10.1016/j.molliq.2016.09.110
23. Y.L. Kobzar and K. Fatyeyeva, Ionic Liquids as Green and Sustainable Steel Corrosion Inhibitors: Recent Developments, Chem. Eng. J., 2021, **425**, 131480. doi: 10.1016/j.cej.2021.131480
24. TM0169/G31-12a, Standard Guide for Laboratory Immersion Corrosion Testing of Metals, NACE International, Houston, TX, USA, 2012.
25. ASTM G 31-72, Standard Guide for Laboratory Immersion Corrosion Testing of Metals, American Society for Testing and Materials, Philadelphia, PA, USA, 1990.
26. T.O. Olomola, S. Durodola, L.O. Olasunkanmi and A. Adekunle, Effect of selected 3-chloromethylcoumarin derivatives on mild steel corrosion in acidic medium: experimental and computational studies, *J. Adhes. Sci. Technol*., 2022, **36**, no. 4, 2547–2561. doi: 10.1080/01694243.2022.2094147

27. A. Alamiery, W.N.R.W. Isahak, H. Aljibori, H. Al-Asadi and A. Kadhum, Effect of the structure, immersion time and temperature on the corrosion inhibition of 4-pyrrol-1-yl-*N*-(2,5-dimethyl-pyrrol-1-yl)benzoylamine in 1.0 M HCl solution, *Int. J. Corros. Scale Inhib*., 2021, **10**, no. 2, 700–713. doi: 10.17675/2305-6894-2021-10-2-14
28. A.Y. Rubaye, A.A. Abdulwahid, S.B. Al-Baghdadi, A.A. Al-Amiery, A.A. Kadhum and A.B. Mohamad, Cheery sticks plant extract as a green corrosion inhibitor complemented with LC-EIS/MS spectroscopy, *Int. J. Electrochem. Sci*., 2015, **10**, no. 10, 8200–8209. doi: 10.1016/S1452-3981(23)11087-X
29. T.A. Salman, A.A. Al-Amiery, L.M. Shaker, A.A.H. Kadhum and M.S. Takriff, A study on the inhibition of mild steel corrosion in hydrochloric acid environment by 4-methyl-2-(pyridin-3-yl)thiazole-5-carbohydrazide, *Int. J. Corros. Scale Inhib*., 2019, **8**, no. 4, 1035–1059. doi: 10.17675/2305-6894-2019-8-4-14
30. A. Al-Amiery, Anti-Corrosion Performance Of 2-Isonicotinoyl-*N*-Phenylhydrazine-carbothioamide For Mild Steel Hydrochloric Acid Solution: Insights From Experimental Measurements And Quantum Chemical Calculations, *Surf. Rev. Lett*., 2021, **28**, no. 3, 2050058. doi: 10.1142/S0218625X20500584
31. M.M. Hanoon, A.M. Resen, L.M. Shaker, A.A.H. Kadhum and A.A. Al-Amiery, Corrosion investigation of mild steel in aqueous hydrochloric acid environment using *N*-(naphthalen-1-yl)-1-(4-pyridinyl)methanimine complemented with antibacterial studies, *Biointerface Res. Appl. Chem*., 2021, **11**, no. 2, 9735–9743. doi: 10.33263/BRIAC112.97359743
32. K.F. Khaled and M.A. Amin, Computational and electrochemical investigation for corrosion inhibition of nickel in molar nitric acid by piperidines, *J. Appl. Electrochem*., 2008, **38**, no. 11, 1609–1621. doi: 10.1007/s10800-008-9604-5
33. A. Elgendy, H. Nady, M.M. El-Rabiei and A.A. Elhenawy, Understanding the adsorption performance of two glycine derivatives as novel and environmentally safe anti-corrosion agents for copper in chloride solutions: Experimental, DFT, and MC studies, *RSC Adv*., 2019, **9**, no. 72, 42120–42131. doi: 10.1039/C9RA08617J
34. E. Karamnia and M. Yousefpour, A study of pomegranate peel extract effect on corrosion inhibition performance on aluminum in HNO_3 solution, *Colloids Surf., A*, 2024, **694**, 134080. doi: 10.1016/j.colsurfa.2024.134080
35. A. Visa, N. Plesu, B. Maranescu, G. Ilia, A. Borota and L. Crisan, Combined Experimental and Theoretical Insights into the Corrosion Inhibition Activity on Carbon Steel Iron of Phosphonic Acids, *Molecules*, 2021, **26**, no. 1 135. doi: 10.3390/molecules26010135
36. T. Hageman and E. Martínez-Pañeda, An electro-chemo-mechanical framework for predicting hydrogen uptake in metals due to aqueous electrolytes, *Corros. Sci*., 2022, **208**, 110681. doi: 10.1016/j.corsci.2022.110681
37. M.A. Quraishi and F.A. Ansari, Imidazole derivatives as corrosion inhibitors for mild steel in acid solutions, Corrosion, 2002, **58**, no. 9, 748–755. doi: 10.5006/1.3287643

38. G. Palumbo, D. Święch and M. Górny, Guar Gum as an Eco-Friendly Corrosion Inhibitor for N80 Carbon Steel under Sweet Environment in Saline Solution: Electrochemical, Surface, and Spectroscopic Studies, *Int. J. Mol. Sci*., 2023, **24**, no. 15, 12269. doi: 10.3390/ijms241512269
39. F. Bentiss, M. Traisnel and M. Lagrenée, The substituted 1,3,4-oxadiazoles: a new class of corrosion inhibitors of mild steel in acidic media, *Corros. Sci*., 2000, **42**, no. 1, 127–146. doi: 10.1016/S0010-938X(99)00049-9
40. I. Ahamad, R. Prasad and M.A. Quraishi, Inhibition of mild steel corrosion in acid solution by phenyl thiourea derivatives: electrochemical and thermodynamic study, *Corros. Sci*., 2010, **52**, no. 9, 3033–3041. doi: 10.1016/j.corsci.2010.05.022
41. K.F. Khaled and M.A. Amin, Corrosion monitoring of mild steel in sulphuric acid solutions in presence of some thiazole derivatives–molecular dynamics, chemical and electrochemical studies, *Corros. Sci*., 2009, 51, no. 9, 1964–1975. doi: 10.1016/j.corsci.2009.05.023
42. A.S. Fouda, A.S. Ellithy and K. Shalabi, Some thiosemicarbazide derivatives as corrosion inhibitors for carbon steel in acidic solution, *Desalination*, 2009, **249**, no. 1, 1081–1090. doi: 10.1016/j.desal.2009.04.028
43. B.E.A. Rani and B.B.J. Basu, Green inhibitors for corrosion protection of metals and alloys: an overview, *Int. J. Corros*., 2012, 380217. doi: 10.1155/2012/380217
44. C. Verma, E.E. Ebenso, M.A. Quraishi and I.B. Obot, Adsorption behavior of glucosamine-based, pyrimidine-fused heterocycles as effective corrosion inhibitors for mild steel in 1 M HCl: insights from electrochemical, thermodynamic and surface characterization studies, *J. Mol. Liq*., 2017, **236**, 139–148. doi: 10.1016/j.molliq.2017.03.085
45. E.E. Ebenso, T. Arslan, F. Kandemirli, N. Caner and I. Love, Quantum chemical studies of some schiff bases as corrosion inhibitors for mild steel in acidic medium, *Int. J. Quantum Chem*., 2010, **110**, no. 5, 1003–1018. doi: 10.1002/qua.22306
46. A.Y. El-Etre, Inhibition of acid corrosion of aluminum using vanillin, *Corros. Sci*., 2001, 43, no. 6, 1031–1039. doi: 10.1016/S0010-938X(00)00127-X
47. R. Solmaz, G. Kardas, M. Culha, B. Yazıcı and M. Erbil, Investigation of adsorption and inhibition effect of 2-mercaptothiazoline on corrosion of mild steel in hydrochloric acid media, *Electrochim. Acta*, 2008, **53**, no. 20, 5941–5952. doi: 10.1016/j.electacta.2008.03.055

♦ ♦ ♦